Available online at www.sciencedirect.com
SCIENCE DIRECT
Current Applied Physics 6 (2006) 525–530
Current Applied Physics
An official journal of the KPS
www.elsevier.com/locate/cap
www.kps.or.kr

Si(0 0 1) surface optical anisotropies induced by π-conjugated overlayers and oxidation

W.G. Schmidt *, A. Hermann, F. Fuchs, F. Bechstedt

Institut für Festkörpertheorie und -optik, Friedrich-Schiller-Universität, Max-Wien-Platz 1, 07743 Jena, Germany

Available online 27 December 2005

Abstract

A density functional (DFT–GGA) study on the modification of the Si(0 0 1) surface optical response upon adsorption of 9,10-phenanthrenequinone and oxidation is presented. In the first case it is found that intramolecular π–π* transitions as well as adsorption-modified Si bulk states contribute to the optical signal. The molecular contributions differ strongly from the respective signals of gas-phase molecules, indicating the need for a cautious interpretation of experimental data. The calculations for oxidized Si structures show that local Si lattice deformations accompanying the oxidation of Si bulk bonds directly at the silicon–silicon oxide interface give rise to pronounced optical anisotropies that explain the experimental findings very well. In contrast, calculations for translationally invariant oxide structures fail to reproduce the experiment. This indicates the oxidation to occur layer-by-layer and strong disorder of the silicon oxide layers immediately above the interface.
© 2005 Elsevier B.V. All rights reserved.

PACS: 78.68.+m; 78.66.Qn

Keywords: Density functional theory; Silicon surface; Organic functionalization; 9,10-Phenanthrenequinone; Silicon surface oxidation; Reflectance anisotropy spectroscopy; Reflectance difference spectroscopy

1. Introduction

Reflection anisotropy (or difference) spectroscopy (RAS/RDS) is a non-destructive optical probe of surfaces that is capable of operation within a wide range of environments [1]. Photons penetrate deeply into the substrate, of the order of 10^3 Å, and the optical anisotropy signal can thus be helpful to explore interfaces buried beneath organic and oxide layers as we will show below.

In the last years, an increasing amount of work has been dedicated to the grafting of organic molecules on the Si(0 0 1) surface [2]. Such hybrid systems open the way for integrating the electronic, optical or biological properties of organic layers in classical silicon-based devices. The structural investigation of these systems by the usual laboratory surface techniques using electrons is a difficult task, because the direct access to the interface is prevented by the presence of the organic adlayer. In contrast, techniques based on photons can be used to study the interface through the adsorbed thin film. Therefore, RAS is increasingly used in this context [3–6]. It does not depend on ultra-high vacuum conditions, and is compatible with truly challenging preparation conditions such as surfaces under liquids. Unfortunately, the interpretation of RAS spectra is difficult and only a few computational studies address the optical response of organic overlayers [7–10]. Therefore, the contribution of organic thin films to the semiconductor surface optical response is essentially unknown, hindering the efficient use of optical spectroscopies for organic layer and interface characterization.

Recently, Hacker and Hamers [5] studied the optical anisotropy of 9,10-phenanthrenequinone ("PQ", $C_{14}O_2H_8$)

* Corresponding author. Fax: +49 5251 603435.
E-mail addresses: wgs@phys.upb.de, W.G.Schmidt@ifto.physik.uni-jena.de (W.G. Schmidt).

1567-1739/$ - see front matter © 2005 Elsevier B.V. All rights reserved.
doi:10.1016/j.cap.2005.11.069

adsorbed on Si(0 0 1) as a prototype for a π-conjugated overlayer system. PQ has two highly reactive carbonyl groups assumed to bond to the surface (''bonding group''), a delocalized π-electron system (''functional group''), and forms a large variety of derivatives. The π-conjugation, likely to remain intact upon adsorption, should allow for direct observation of intramolecular as well as interface- and substrate-related transitions in the experimentally accessible photon energy range [11]. Indeed, a pronounced RAS feature was measured for photon energies of about 5.2 eV and assigned to such intramolecular π–π* transitions. Here we use the adsorption of PQ to analyze in detail the optical response of an organic monolayer on Si(0 0 1).

Despite decades of effort, the mechanism of the Si(0 0 1) surface oxidation as well as the microscopic structure of the silicon/silicon oxide interface are still under discussion, see, e.g., Ref. [12]. RAS spectra measured during thermal oxide growth show oscillations, i.e, repeated changes of the optical anisotropy polarity, for photon energies around the E_1 and E_2 critical points (CPs) of bulk Si as well as above 5 eV [13–15]. Scanning reflection electron microscopy [16] and total-energy calculations [17] indicate that the thermal oxidation of Si(0 0 1) proceeds layer-by-layer. This suggests to relate the optical anisotropy oscillations to the layer oxidation. However, previous numerical simulations based on ordered oxidized Si(0 0 1) surfaces [6,18–20] failed to explain the measured data and their relation to the interface structure. Here we follow a somewhat different approach and in addition to ordered interfaces also simulate the optical anisotropy due to oxidized Si bulk bonds underneath a disordered silicon oxide layer.

2. Methodology

The calculations are based on the gradient-corrected density functional theory (DFT–GGA) [21], as implemented in the VASP package [22]. Periodically repeated $p(4\times2)$ and $p(2\times2)$ supercells model the surface. The reflectance anisotropy is calculated according to the scheme devised by Del Sole [23], with computational details similar to Ref. [9]: the slab polarizability is obtained within independent-particle approximation from all-electron wave functions obtained using the projector-augmented wave (PAW) method [24]. Excitonic and local-field effects [25] are neglected. We apply a rigid energy shift of 0.5 eV to the conduction bands in order to account for the DFT band-gap under-estimation. This value leads to a good agreement between the calculated and measured bulk critical point energies of Si. Fortuitously, it is nearly appropriate also for gas-phase PQ. RAS spectra are difference spectra, which are furthermore normalized to the bulk dielectric function. Therefore, calculations within the independent-particle approximation reliably reproduce experimental data for a wide range of semiconductors [26].

3. Results and discussion

3.1. Phenanthrenequinone adsorbed on Si(0 0 1)

Experiment [27] and total-energy calculations [10] indicate that the molecules bond via their carbonyl groups to the Si dimer, forming a [4 + 2] Diels–Alder product. The optimized geometry is shown in Fig. 1. It features PQ molecules that arrange in zig-zag chains on the surface and co-adsorbed hydrogen at the remaining Si dimer atoms. This configuration is used below for optical-response calculations.

The reflectance anisotropy calculated for PQ molecules adsorbed on Si(0 0 1) (solid curve in Fig. 2) is in good agreement with the measured data [5]. Compared to the spectrum of the clean surface (see, e.g., Refs. [28,29]), new optical anisotropies show up. Among these, the B_1 feature at about 5.2 eV is the most pronounced one.

In order to determine the origin of these interface optical anisotropies, the valence orbitals of the supercell are classified with respect to their localization either below or above the Si surface: an electronic state is classified as molecular state if the state density integrate above the vertical position of the uppermost Si atom is more than 70% of the total integrated density. This decomposition allows for the separation of the substrate and organic layer contributions to the total optical signal. The respective RAS spectra are shown by the dashed lines in Fig. 2. Obviously, bulk contributions dominate the optical signal. The RAS features at the E_1 and E_2 Si bulk critical points as well as the B_1 and B_2 features arise from transitions involving Si bulk states. This is in clear contrast to the interpretation of the B_1 feature as due to molecular π–π* transitions [5]. Therefore, we perform additional calculations: the adsorbed PQ molecules are replaced by two OH groups each. By keeping the slab geometry (including the O atoms) fixed, the RAS contribution of the strained and rebonded substrate can be calculated. The obtained spectrum (bottom curve in Fig. 2) reproduces all main features of the Si substrate signal, i.e., the E_1/E_2 features as well as B_1 and B_2. Evidently, B_1 and B_2 do not arise from molecular transitions but are

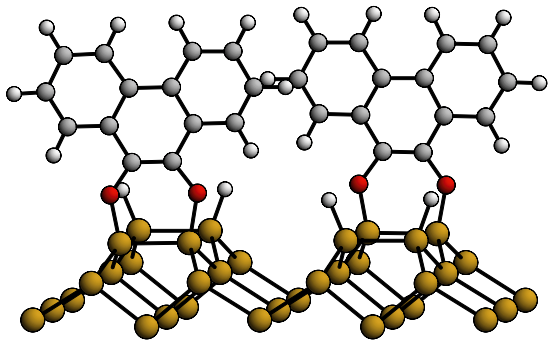

Fig. 1. Structural model for PQ adsorption on Si(0 0 1). Large (red/dark, grey, light) circles denote Si (O, C, H) atoms, respectively. (For interpretation of the references in colour in this figure legend, the reader is referred to the web version of this article.)

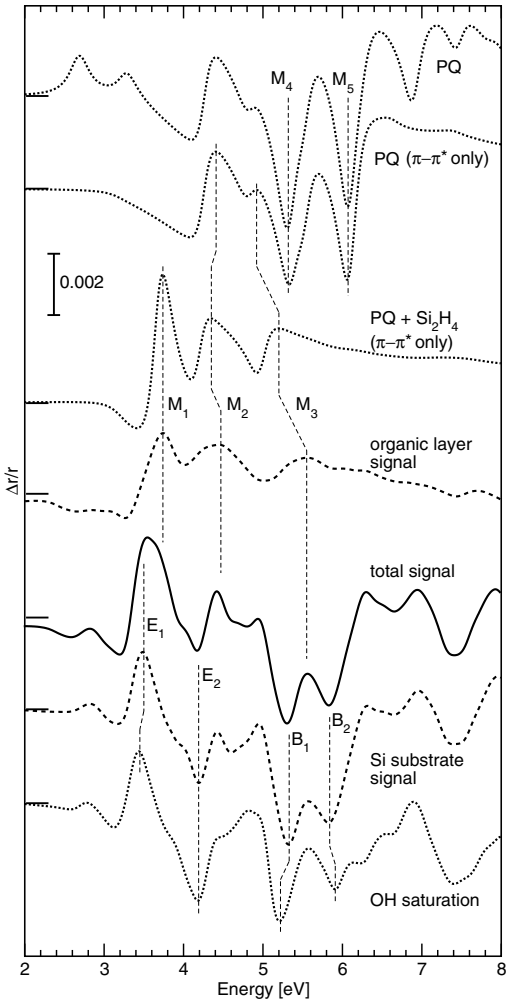

Fig. 2. Total calculated RAS spectrum [$\mathrm{Re}\{(r_{[\bar{1}10]} - r_{[110]})/\langle r\rangle\}$] and its decomposition into overlayer and bulk contributions (see text).

clearly due to adsorption-induced distortions of the substrate. We find that both the adsorption-induced strain in the silicon lattice and the formation of Si–O bonds contribute to these anisotropies.

Although less pronounced than expected, there are also RAS contributions to the total signal that originate in the organic layer as shown in Fig. 2: the total signal is modified by molecular transitions denoted M_1, M_2, and M_3. What is the origin of these features? To answer this question we simulate the RAS response of an organic overlayer on top of optically isotropic Si by using the three-layer model shown in the inset of Fig. 3. This model allows for simulating the optical response as a function of the organic layer constituents. The topmost RAS curve in Fig. 2 is obtained by assuming the organic layer to consist of PQ molecules that have an optical absorption equal to their gas-phase spectrum. Interestingly, the calculated RAS spectrum shows pronounced π–π* transition-related M_4 and M_5 features that nearly coincide in energy with the B_1 and B_2 peaks measured by Hacker and Hamers [5]. However, the RAS obtained from the fictitious layer of gas-phase PQ molecules clearly fails to reproduce the calculated organic layer contribution to the total signal (upper dashed curve in Fig. 1). This is expected: the carbonyl group-related transitions will vanish or at least be shifted to much higher energies upon molecular adsorption. Therefore, in a second step, we calculate the RAS as above, but restrict the optical response to π–π* transitions of the gas-phase molecule. The result, however, agrees only slightly better with the organic layer contribution to the total RAS. To model the bonding with the Si substrate, we therefore construct in a third step an artificial PQ + Si_2H_4 molecule (see Fig. 3), using the atomic coordinates from the calculated adsorption geometry. The Si–O bonding leads to a charge redistribution in the molecule and to the formation of a new C=C double bond (V_1 in Fig. 3) between the carbonyl group C atoms, which corresponds now to the highest occupied molecular orbital (HOMO). By restricting the calculation to transitions between the three highest occupied π-orbitals and the two lowest unoccupied π*-orbitals one obtains the third curve of Fig. 1. Obviously, the line shape and peak positions of the organic layer signal are well described by such a model for the constituents of the organic film. Thus, the essential parts of the molecular contributions to the RAS can be traced back to a few π–π* transitions within the PQ molecule. However, the bonding to the substrate must be taken into account: the feature M_1 arises solely from transitions involving the C=C double bond which forms as a result of the [4 + 2] Diels–Alder reaction with the Si=Si dimer. At the same time, the formerly pronounced M_4 and M_5 features are strongly reduced in amplitude and shifted in energy, due to the substrate-bonding related changes of the respective molecular orbitals. Fig. 3 shows the molecular states responsible for the RAS features related to the organic overlayer: M_1, M_2, and M_3 stem from V_1–C_2, V_2–C_1, and V_3–C_1 transitions, respectively.

3.2. Oxidized Si(001) surfaces

Fig. 4 shows schematically the clean Si(001) surface and an energetically favored geometry used to model the oxidation of the first Si layer [30]. The bottom curve in Fig. 5 shows the reflectance anisotropy calculated for the clean Si(001)$c(4\times2)$ surface. It is characterized by a strong, dimer-state related minimum at 1.7 eV. An additional minimum/maximum structure slightly below/above the E_1/E_2 CP energy of bulk Si at 3.5/4.3 eV results from surface-modified bulk states. The calculated spectrum agrees with the data measured for highly oriented, single-domain Si(001) surfaces [28,15].

Upon oxidation, the reflectance anisotropy of the clean surface changes strongly. The 1.7 eV feature is quenched, due to the saturation of the Si-dimer states. In Fig. 5 we show the measured RAS data assigned to the complete oxidation of the first atomic monolayer [13]. It is positive for all photon energies considered, with maxima close to the E_1 and E_2 CPs and at about 5.3 eV. RAS calculations based on translationally invariant models of oxidized Si(001)

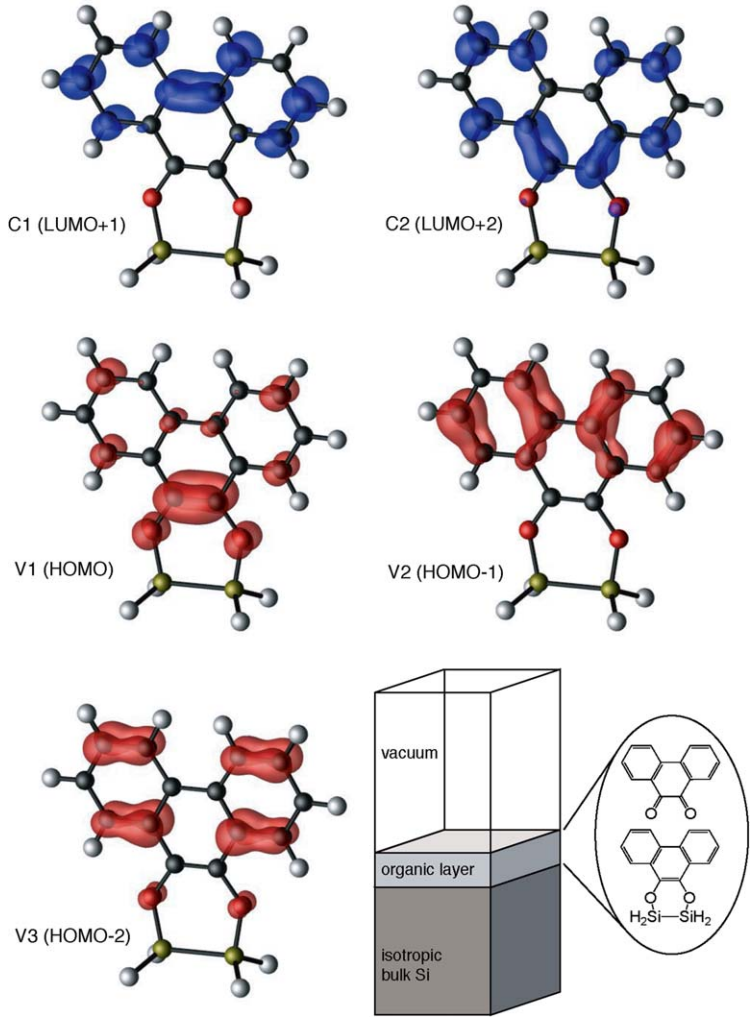

Fig. 3. Relevant molecular orbitals of the PQ + Si_2H_4 molecule (see text). The three-layer model for simulating "simplified" RAS spectra is shown as inset.

surfaces only explain part of the measured features. The oxidation model shown in Fig. 4 gives rise to an optical anisotropy that is positive throughout the energy range probed. However, there are clear deviations between experiment and theory. The discrepancies between experiment and theory are even more pronounced for RAS calculations based on ordered surface structures different from the model shown in Fig. 4 [6,19,20].

The top curve in Fig. 5 shows experimental data assigned to the oxidation of the second monolayer [13]. Nearly an inversion of the signal is observed, compared to the spectrum assigned to the oxidation of the first monolayer (this inversion occurs repeatedly during the progression of the oxidation, see Ref. [15]). Negative anisotropies occur for photon energies close to the Si bulk CPs and above 4.5 eV. We failed completely to reproduce this spectrum using any of the structural models proposed for oxidation of the uppermost two atomic layers of Si(0 0 1) [30]. Strong deviations from experiment occur in all cases.

Surface disorder not contained in the translationally invariant oxidation models could possibly explain the failure of the calculations. That oxidation causes considerable surface disorder is in accord with high-energy electron diffraction data [16] and scanning tunneling microscopy images of Si(0 0 1) surfaces exposed to oxygen [31]. Bulk Si is optically isotropic. If the disorder of the oxide film above the interface renders this film optically isotropic too, the only source of optical anisotropy are oxygen atoms inserted into Si–Si bulk bonds directly at the interface. Therefore, the optical anisotropy induced by oxygen inserted into bulk Si bonds is investigated, using an orthorombic supercell with $2 \times 2 \times 20$ periodicities along the $[\bar{1}\,1\,0]$, $[1\,1\,0]$, and $[0\,0\,1]$ directions, respectively. The difference of the $[\bar{1}\,1\,0]$ and $[1\,1\,0]$ bulk polarizability components is normalized such as to compare with the surface reflectance anisotropy. The results for Si–O–Si bonds in $(\bar{1}\,1\,0)$ and $(1\,1\,0)$ planes (shown in Fig. 5) reproduce the major features measured after oxidation of the first and second monolayer, respectively. Given the simplicity of this idealized model, the agreement between calculation and measurement is impressive. The measured RAS oscillations are thus explained naturally by assuming that (i) the

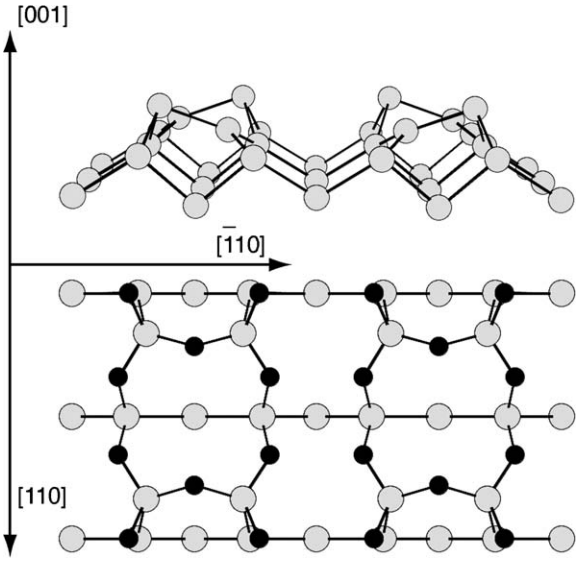

Fig. 4. Perspective view of the clean relaxed Si(0 0 1)$c(4\times2)$ surface (top), and top view of a structural model for the oxidation of the first Si(0 0 1) layer (bottom). Dark and grey symbols indicate O and Si atoms, respectively.

oxidation occurs layer-by-layer and (ii) the silicon oxide directly above the abrupt interface is disordered and therefore optically isotropic.

After having reproduced the experimental data by calculations for oxidized Si bulk, we investigate the origin of the optical anisotropies in more detail. Earlier measurements of the Si–SiO_2 interface optical properties have often been interpreted in terms of strain-induced shifts of the Si bulk CP energies [32–34]. We perform model calculations for 4 Si bulk layers uniformly strained by 2% along [1 1 0], a value that roughly accounts for the lattice compression around an oxygen atom inserted into a Si(0 0 1)(2×2) interface unit cell. As seen in the inset of Fig. 5, the optical anisotropy induced by such a macroscopic strain accounts for the sign and roughly for the magnitude of the measured signal, but does not reproduce the line shape. Therefore, either the Si–O bond-related electronic states or the complicated local deformation pattern must cause the peculiar features at E_1 and E_2. Based on a detailed analysis of the transition matrix elements contributing to the total RAS signal, we can exclude the first possibility: the optical anisotropies are caused be a multitude of perturbed Si bulk states. To corroborate the second hypothesis we perform calculations using the frozen lattice deformation pattern around an inserted oxygen, but replacing the O atom with two H atoms for Si dangling bond termination (cf. "local strain pattern" curve in Fig. 5). Indeed, a line shape is obtained that agrees well with the oxygen inserted case, at least around E_1 and E_2. This shows that the strain is indeed causing the optical anisotropy. However, it is important to account for the *local* deformation pattern around the defect. An uniform compression is not sufficient to model the measured RAS. Fig. 6 illustrates the complexity of the Si bulk deformation around an oxidized Si bond.

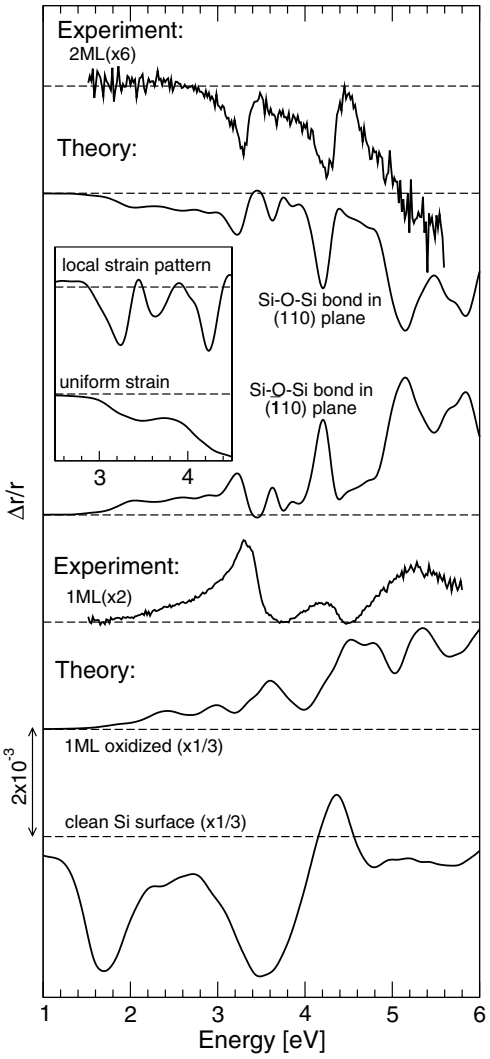

Fig. 5. RAS spectra [Re$\{(r_{[\bar{1}10]} - r_{[110]})/\langle r\rangle\}$] calculated for the oxidized Si(0 0 1) configuration shown in Fig. 4, the clean Si(0 0 1)$c(4\times2)$ surface, and modified Si bulk structures (see text) are compared with measured data for one and two monolayer oxidation [13].

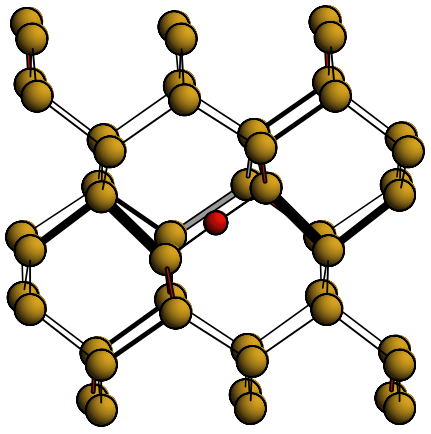

Fig. 6. Calculated lattice deformation around an oxidized Si bond within a $2\times2\times20$ supercell. Compressive (tensile) strain is indicated by black (grey) bonds, with the thickness of the bonds indicating the amount of local strain. Large and small symbols indicate Si and O atoms, respectively.

4. Conclusions

In conclusion, the influence of an organic layer on the optical properties of the Si(0 0 1) surface has been analyzed using *first-principles* calculations. Strong modifications of the intramolecular transitions are found even for a molecule like 9,10-phenanthrenequinone, where bonding and functional groups are seemingly decoupled. This shows that a naive interpretation of the surface optical response in terms of molecular transitions fails. On the other hand, the optical anisotropy of the substrate is significantly altered. The total spectrum is dominated by contributions from adsorption-modified Si bulk states.

We also calculated the optical response of oxidized and strained silicon structures. Comparison of the simulated optical spectra with experiment indicates that (i) the measured oscillations of the optical anisotropy during oxidation are caused by the progression of the local strain pattern during the oxidation, (ii) the oxide layer directly above the interface is disordered and (iii) the oxidation proceeds layer-by-layer and there exists an one-to-one correspondence between the layer oxidation and the inversion of the interface optical anisotropy.

Our results thus suggest optical spectroscopy for monitoring and controlling the oxidation process with atomic resolution as well as for characterizing organic–inorganic interfaces.

Acknowledgements

Grants of computer time from the Leibniz-Rechenzentrum München and the Höchstleistungsrechenzentrum Stuttgart are gratefully acknowledged. We thank the Deutsche Forschungsgemeinschaft for financial support (SCHM-1361/6).

References

[1] P. Weightman, D.S. Martin, R.J. Cole, T. Farrel, Rep. Prog. Phys. 68 (2005) 1251.
[2] R.A. Wolkow, Annu. Rev. Phys. Chem. 50 (1999) 413.
[3] A. Sassella, A. Borghesi, F. Meinardi, R. Tubono, M. Gurioli, C. Botta, W. Porzio, G. Barbarella, Phys. Rev. B 62 (2000) 11170.
[4] A.M. Paraian, U. Rossow, S. Park, G. Salvan, M. Friedrich, T.U. Kampen, D.R.T. Zahn, J. Vac. Sci. Technol. B 19 (2001) 1658.
[5] C.A. Hacker, R.J. Hamers, J. Phys. Chem. B 107 (2003) 7689.
[6] W.G. Schmidt, F. Fuchs, A. Hermann, K. Seino, F. Bechstedt, R. Paßmann, M. Wahl, M. Gensch, K. Hinrichs, N. Esser, S. Wang, W. Lu, J. Bernholc, J. Phys.: Condens. Matter 16 (2004) S4323.
[7] W. Lu, W.G. Schmidt, J. Bernholc, Phys. Rev. B 68 (2003) 115327.
[8] P. Silvestrelli, O. Pulci, M. Palummo, R. Del Sole, F. Ancilotto, Phys. Rev. B 68 (2003) 235306.
[9] K. Seino, W.G. Schmidt, Surf. Sci. 548 (2004) 183.
[10] A. Hermann, W. Schmidt, F. Bechstedt, J. Phys. Chem. B 109 (2005) 7928.
[11] B.G. Frederick, J.R. Power, R.J. Cole, C.C. Perry, Q. Chen, S. Haq, T. Bertrams, N.V. Richardson, P. Weightman, Phys. Rev. Lett 80 (1998) 4490.
[12] J. Dabrowski, H.-J. Müssig, Silicon Surfaces and Formation of Interfaces, World Scientific, Singapore, 2000.
[13] T. Yasuda, S. Yamasaki, M. Nishizawa, N. Miyata, A. Shklyaev, M. Ichikawa, T. Matsudo, T. Ohta, Phys. Rev. Lett. 87 (2001) 037403.
[14] T. Yasuda, N. Kumagai, M. Nishizawa, S. Yamasaki, H. Oheda, K. Yamabe, Phys. Rev. B 67 (2003) 195338.
[15] T. Yasuda, M. Nishizawa, N. Kumagai, S. Yamasaki, H. Oheda, K. Yamabe, Thin Solid Films 455–456 (2004) 759.
[16] H. Watanabe, K. Kato, T. Uda, K. Fujita, M. Ichikawa, T. Kawamura, K. Terakura, Phys. Rev. Lett. 80 (1998) 345.
[17] H. Kageshima, K. Shiraishi, Phys. Rev. Lett. 81 (1998) 5936.
[18] T. Nakayama, M. Murayama, Appl. Phys. Lett. 77 (2000) 4286.
[19] A. Incze, R. Del Sole, G. Onida, Phys. Rev. B 71 (2005) 035350.
[20] F. Fuchs, W.G. Schmidt, F. Bechstedt, J. Phys. Chem. B 109 (2005) 17649.
[21] J.P. Perdew, J.A. Chevary, S.H. Vosko, K.A. Jackson, M.R. Pederson, D.J. Singh, C. Fiolhais, Phys. Rev. B 46 (1992) 6671.
[22] G. Kresse, J. Furthmüller, Comp. Mat. Sci. 6 (1996) 15.
[23] R. Del Sole, Solid State Commun. 37 (1981) 537.
[24] G. Kresse, D. Joubert, Phys. Rev. B 59 (1998) 1758.
[25] P.H. Hahn, W.G. Schmidt, F. Bechstedt, Phys. Rev. Lett. 88 (2002) 016402.
[26] W.G. Schmidt, F. Bechstedt, J. Bernholc, J. Vac. Sci. Technol. B 18 (2000) 2215.
[27] L. Fang, J. Liu, S. Coulter, X. Cao, M.P. Schwartz, C. Hacker, R.J. Hamers, Surf. Sci. 514 (2002) 362.
[28] R. Shioda, J. van der Weide, Phys. Rev. B 57 (1998) R6823.
[29] W.G. Schmidt, F. Bechstedt, J. Bernholc, Phys. Rev. B 63 (2001) 045322.
[30] T. Yamasaki, K. Kato, T. Uda, Phys. Rev. Lett. 91 (2003) 146102.
[31] K. Fujita, H. Watanabe, M. Ichikawa, Appl. Phys. Lett. 70 (1997) 2807.
[32] J.T. Fitch, C.H. Bjorkman, G. Lucovsky, F.H. Pollak, X. Yin, J. Vac. Sci. Technol. B 7 (1989) 775.
[33] Z. Yang, Y.H. Chen, J.Y.L. Ho, W.K. Liu, X.M. Fang, P.J. McCann, Appl. Phys. Lett. 71 (1997) 87.
[34] W. Daum, H.-J. Krause, U. Reichel, H. Ibach, Phys. Rev. Lett. 71 (1993) 1234.